

A MECHANISTIC THEORY FOR HEAT TRANSFER BETWEEN FLUIDIZED BEDS OF LARGE PARTICLES AND IMMERSED SURFACES

V. L. GANZHA

Luikov Heat and Mass Transfer Institute, B.S.S.R. Academy of Sciences, Minsk, B.S.S.R., U.S.S.R.

and

S. N. UPADHYAY* and S. C. SAXENA

Department of Energy Engineering, University of Illinois at Chicago Circle, Box 4348, Chicago, IL 60680,
 U.S.A.

(Received 26 November 1981)

Abstract A mechanistic theory for the heat transfer between an immersed surface and a fluidized bed of large particles is developed by adopting the well accepted concept that in the absence of radiation the total heat transfer coefficient is the sum of conductive (h_{cond}) and convective (h_{conv}) components. The solids are assumed to be distributed around the heat transfer surface in an arrangement of unit orthorhombic cells. h_{cond} is then computed by considering a composite infinite layer of gas and solid and by solving the unsteady state heat conduction equations under well defined boundary and initial conditions. h_{conv} is evaluated by assuming that the turbulent boundary layer on the heat transfer surface is disrupted at the front half of the particle and is reformed in its wake. The theoretical model predictions for the total heat transfer coefficient are in good agreement with the available experimental data on large particle systems. The proposed theory is considered a good predictive and design tool.

NOMENCLATURE

a ,	a function of $\bar{\epsilon}$ and ϵ_w in equation (46);	$h_{w,\text{max}}$	maximum heat transfer coefficient [W m ⁻² K ⁻¹];
Ar ,	Archimedes number $\bar{d}_p^3 g \rho_g (\rho_p - \rho_g) / \mu_g^2$;	k ,	gas film thickness defined by equation (32) [m];
C ,	a constant in equation (35);	k_g ,	thermal conductivity of gas [W m ⁻¹ K ⁻¹];
C_{pg} ,	specific heat of gas at constant pressure [J kg ⁻¹ K ⁻¹];	k_p ,	thermal conductivity of particle [W m ⁻¹ K ⁻¹];
C_{pp} ,	specific heat of particle at constant pressure [J kg ⁻¹ K ⁻¹];	K_1 ,	dimensionless thermal conductivity ratio, (k_g/k_p);
C_0 ,	a constant in equation (40);	K_2 ,	dimensionless thermal diffusivity ratio, (α_g/α_p);
d_c ,	equivalent cylinder diameter [m];	K_δ ,	dimensionless ratio, [$k_g C_{pg} \rho_g / k_p C_{pp} \rho_p$];
d_p ,	average particle diameter [m];	K_δ ,	dimensionless thickness ratio, (d_c/δ);
D_T ,	tube diameter [m];	l ,	characteristic length parameter [m];
Fo ,	Fourier number for gas film, ($\alpha_g \tau / \delta^2$);	L ,	center-center distance between adjacent equivalent cylinders [m];
Fo_1 ,	Fourier number for particle, ($\alpha_p \tau / d_c^2$);	m ,	dimensionless function, ($K_1^{1/2} K_2$);
g ,	acceleration due to gravity [m s ⁻²];	N ,	number of particles per unit area of the heat transfer surface;
G ,	superficial mass flow velocity [kg m ⁻² s ⁻¹];	Nu_{cond} ,	conductive component of particle Nusselt number ($h_{\text{cond}} \bar{d}_p / k_g$);
G_{mf} ,	mass flow velocity at minimum fluidizing condition [kg m ⁻² s ⁻¹];	Nu_{conv} ,	convective component of particle Nusselt number ($h_{\text{conv}} \bar{d}_p / k_g$);
h ,	thickness of segment of particle [m];	Nu_{conv} ,	convective Nusselt number based on characteristic length parameter, ($h_{\text{conv}} l / k_g$);
h_c ,	thickness of segment of tube [m];	Nu_p ,	particle Nusselt number, ($h_w \bar{d}_p / k_g$);
h_{cond} ,	conductive component of heat transfer coefficient [W m ⁻² K ⁻¹];	Pr ,	Prandtl number, ($\mu_g C_{pg} / k_g$);
h_{conv} ,	convective component of heat transfer coefficient [W m ⁻² K ⁻¹];	q ,	heat flux [W m ⁻²];
h_w ,	average heat transfer coefficient [W m ⁻² K ⁻¹];	Re ,	Reynolds number, ($\bar{d}_p G / \mu_g$);
		Re_p ,	Reynolds number based on characteristic

* Permanent address: Department of Chemical Engineering, Institute of Technology, Banaras Hindu University, Varanasi-221005, India

	length parameter, (lG/μ_g) ;
Re_{mf} ,	Reynolds number at minimum fluidizing condition, $(\bar{d}_p G_{mf}/\mu_g)$;
T_b ,	bulk bed temperature [K];
T_f ,	normalized temperature of the particle on the bed side [K];
T_g ,	instantaneous temperature of gas film [K];
T_{gp} ,	average temperature of gas-particle composite layer [K];
T_p ,	instantaneous temperature of particle [K];
T_s ,	surface temperature [K];
T_w ,	normalized temperature of heat transfer surface [K];
x ,	space coordinate [m];
y ,	space coordinate [m].
Greek symbols	
α_g ,	thermal diffusivity of gas, $(k_g/C_{pg}\rho_g)$ [$m^2 s^{-1}$];
α_p ,	thermal diffusivity of particle, $(k_p/C_{pp}\rho_p)$ [$m^2 s^{-1}$];
δ ,	gas film thickness for flat surface [m];
δ_c ,	gas film thickness for curved surface [m];
ε ,	bed voidage near heat transfer surface;
$\bar{\varepsilon}$,	bulk bed voidage at minimum fluidization;
ε_w ,	bed voidage near heat transfer surface at minimum fluidization;
θ_g ,	dimensionless temperature for gas as defined by equation (11);
θ_p ,	dimensionless temperature for particle as defined by equation (12);
μ ,	a quantity defined by equation (15);
μ_1, μ_n ,	characteristic roots of equation (15);
μ_g ,	viscosity of gas [$kg m^{-1} s^{-1}$];
ρ_g ,	density of gas [$kg m^{-3}$];
ρ_p ,	density of particle [$kg m^{-3}$];
τ ,	time [s];
τ_1 ,	residence time of particle on the surface [s].

INTRODUCTION

THE NEED to exploit efficiently coal and other solid fuels to generate energy has come as a serious challenge to engineers. To accomplish this, fluidized-bed combustion of coal has emerged as an efficient and environmentally acceptable technology. The various technical details of this concept have not yet been developed to a stage where reliable operations and economic gains in commercial units may be ensured. The design of heat transfer surfaces to be immersed in the bed is one such area which needs thorough understanding. There is an abundance of experimental data of this nature mostly taken on beds of small sizes with small particles under ambient conditions of temperature and pressure. The details of these investigations and the efforts to understand the associated heat transfer mechanisms are reported and

discussed in several recent texts [1-4]. However, in large scale combustors the bed particles are sufficiently large (> 1 mm), and the temperatures and pressures are also much higher than the ambient. The fluidization characteristics of such beds are much different from beds of small particles operating at or near ambient conditions [5]. In large particle fluidized beds, the gas flow is in turbulent regime and the bubbling phenomenon which plays such an important role in small particle systems is found to be much less significant [6]. In view of this a few theoretical [8-13] and experimental [8, 9, 11, 13-15] studies have been undertaken involving heat transfer in large particle fluidized beds with immersed simulated boiler tubes.

Zabrodsky *et al.* [13] found that their data on heat transfer coefficients with horizontal tube bundles immersed in fluidized beds of millet and fire clay could not be reproduced with the theories of Glicksman and Decker [12] and Staub [10]. A similar conclusion emerged from a later study of Borodulya *et al.* [14]. It may be noted that these studies [13, 14] involve two different sets of experimental data taken on two different units. Further, these two studies also revealed that the theory given by Zabrodsky *et al.* [13] gives a relatively superior reproduction of experimental data [13, 14]. Catipovic *et al.* [11] have more recently advanced a theory and compared its predictions with their data on single tube and tube bundles in fluidized beds of large particles. The agreement between theory and experiment was found to be good only at high fluidizing velocity. However, all the three theories [10-12] fail to reproduce the correct dependence of heat transfer coefficient on fluidizing velocity. The theories predict it to decrease monotonically as the fluidizing velocity is increased while the experiments yield a maximum. The theory of Zabrodsky *et al.* [13] does lead to such a trend but the maximum is much less sharp than the observed one. Our yet unpublished work indicates that all these four theories are incapable of reproducing heat transfer data for pressurized systems, and even at ambient pressures for high temperatures.

With the aim being to develop a general mechanistic theory for the heat transfer process in large particle fluidized beds which may not suffer from the above mentioned deficiencies, the present work is undertaken. The model described here neglects radiation and regards the heat transfer coefficient as composed of gas conduction and convection terms. It is assumed that particles on the heat transfer surface are arranged in an orthorhombic arrangement. It is further assumed that particles can be replaced by equivalent cylinders having the same volume as the actual particles and of equal height and diameter. The conduction contribution is calculated by computing the unsteady state heat transfer rate from the surface to the first layer of particles through the gas film or lens enclosed between the two. The convection contribution is obtained by assuming that a turbulent boundary layer on the heat transfer surface is continuously disrupted by the solid

particles and by considering the analogy of this process with that of a flat plate immersed in a solids-free turbulent gas stream. The mathematical description of the model and a comparison of its predictions with the available experimental data are also given here. A preliminary report of some of the aspects of the present model has already been presented [17].

THE HEAT TRANSFER MODEL

It is generally accepted that bed-surface heat transfer is composed of three components: conduction, convection and radiation. At temperatures lower than about 1100K the available information suggests that the effect of radiation is negligible [18]. Consequently, the heat transfer coefficient can be represented as

$$h_w = h_{\text{cond}} + h_{\text{conv}} \quad (1)$$

For fine particles, the component h_{cond} contributes more to h_w than h_{conv} , while for coarse particles the magnitudes of h_{cond} and h_{conv} are comparable. The fine and coarse particles for our present discussion may be taken as corresponding to Group A and Group B powders respectively of ref. [19]. For still larger particles, Group D powders of ref. [19], h_{conv} becomes more pronounced than h_{cond} . The dependence of h_{conv} on pressure is somewhat involved inasmuch as it depends on the particle size, as shown by some recent experimental work [15-17, 20]. It is shown that for all sizes of particles the heat transfer coefficient increases with pressure, the increase is much more for larger particles than for smaller particles. The increase for small particles is due to the improvement in bed structure and hydrodynamics with increasing pressure whereas for larger particles the increase in h_w is due to the enhancement in the component h_{conv} of h_w .

Calculation of conductive component, h_{cond}

There are many models which have been proposed for the calculation of h_{cond} . Many of these models are quite complicated and involve parameters which are difficult to establish. For large particle fluidized beds, the contribution of h_{cond} to h_w being small, it will be

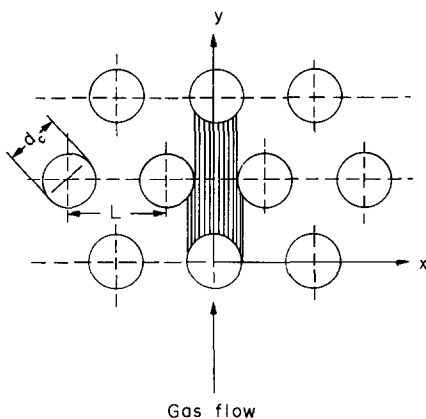


FIG. 1. Orthorhombic particle arrangement on the heat transfer surface.

sufficient to evolve a model which is simple and involves parameters which can be easily determined. We therefore assume that there exists an orthorhombic arrangement of particles around the heat transfer surface (Fig. 1). It is further assumed to simplify the formulation that the particles can be replaced by equivalent cylinders whose volumes are the same as those of the particles and of unit diameter to height ratio. The diameter of these equivalent cylinders, d_c , is related to the particle diameter, d_p , by

$$d_c = (2/3)^{1/3} \bar{d}_p \quad (2)$$

The orthorhombic arrangement of particles around the surface can be considered as a repetition of a unit orthorhombic cell formed by four adjacent particles with center-center interparticle separation of L (Fig. 1). L and d_p are interrelated such that

$$L = \bar{d}_p \left(\frac{1 - \bar{\epsilon}}{1 - \epsilon} \right)^{1/3} \quad (3)$$

where $\bar{\epsilon}$ and ϵ are the bed voidages at minimum fluidization and any other velocity respectively. For fixed bed voidage which is the same as the minimum fluidization voidage, $\bar{\epsilon}$ is computed for an orthorhombic arrangement of particles as 0.395.

For large particle systems, it is a good approximation to assume that all the resistance to heat transfer is confined to the first row of particles near the heat transfer surface only. The heat is transferred by conduction through the gas lens between the surface and the particle. To be consistent with our equivalent volume cylinder assumption concerning the particles, it is logical to regard that the gas-lens has a diameter equal to that of the equivalent cylinder, d_c , and we further assume that it has a uniform thickness of δ . This latter assumption is adopted here for simplicity. Later we also consider the curvature of the heat transfer surface. Thus the heat transfer problem to be considered is that of conduction through a composite layer of gas of thickness δ and of solid of thickness d_c . Let the temperature of the heat transfer surface and the bed be T_s and T_b respectively. Furthermore if there are no temperature-jump effects at the gas-solid interface, it is reasonable to regard the temperature of the gas film heat transfer surface interface as T_s and the temperature of the particle surface facing the bed as T_b . The instantaneous temperature profiles for such a composite layer of gas and solid particle are shown in Fig. 2. Representing the temperatures relative to T_b , gives the heat transfer surface temperature as $T_w = (T_s - T_b)$, and that for the particle surface on the bed side as $T_f = (T_b - T_b) = 0$. The heat conduction equations for such a case have been solved [21] and these are

$$\frac{\partial T}{\partial \tau} = \alpha_g \frac{\partial^2 T_g}{\partial x^2} \quad \text{for } \tau > 0, -\delta \leq x \leq 0, \quad (4)$$

$$\frac{\partial T}{\partial \tau} = \alpha_p \frac{\partial^2 T_p}{\partial x^2} \quad \text{for } \tau > 0, 0 \leq x \leq d_c. \quad (5)$$

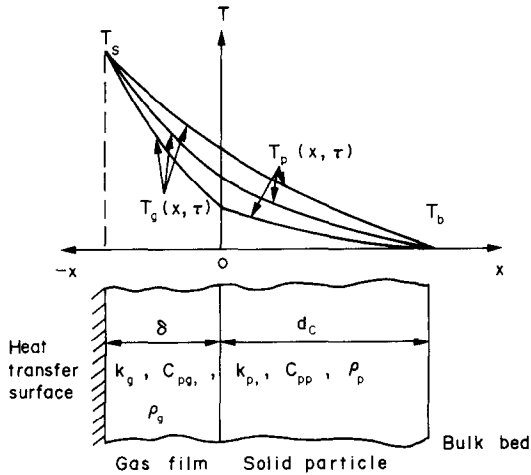


FIG. 2. Transient temperature profiles in the gas-particle composite layer.

The initial and boundary conditions are

$$T_g(x, 0) = T_p(x, 0) = 0, \tag{6}$$

$$T_g(-\delta, \tau) = T_w, \tag{7}$$

$$T_g(0, \tau) = T_p(0, \tau), \tag{8}$$

$$k_g \frac{\partial T_g(0, \tau)}{\partial x} = k_p \frac{\partial T_p(0, \tau)}{\partial x} \tag{9}$$

and

$$T_p(d_c, \tau) = 0. \tag{10}$$

The solutions of these equations are [21]

$$\theta_g = \frac{T_g(x, \tau)}{T_w} = \frac{K_1 d_c - x}{K_1 d_c + \delta} - \sum_{n=1}^{\infty} \times \frac{2K_e \sin^2 m \mu_n \sin[\mu_n(x + \delta)/\delta]}{\mu_n [K_e \sin^2 m \mu_n + m \sin^2 \mu_n]} \times \exp(-\mu_n^2 Fo), \tag{11}$$

$$\theta_p = \frac{T_p(x, \tau)}{T_w} = \frac{d_c - x}{d_c + (\delta/K_1)} - \sum_{n=1}^{\infty} \frac{2K_e [\sin \mu_n \sin K_2^{1/2} K_\delta \mu_n \sin K_2^{1/2} (K_\delta - (x/\delta)) \mu_n]}{\mu_n [K_e \sin^2 K_2^{1/2} K_\delta \mu_n + K_2^{1/2} K_\delta \sin^2 \mu_n]} \times \exp(-\mu_n^2 K_2 K_\delta^2 Fo_1) \tag{12}$$

where

$$K_1 = \frac{k_g}{k_p}; K_e = \left(\frac{k_g C_{pg} \rho_g}{k_p C_{pp} \rho_p} \right)^{1/2}; m = K_2^{1/2} K_\delta \tag{13}$$

$$K_2 = \frac{\alpha_g}{\alpha_p}; K_\delta = \frac{d_c}{\delta}; Fo = \frac{\alpha_g \tau}{\delta^2}; Fo_1 = \frac{\alpha_p \tau}{d_c^2}, \tag{14}$$

and μ_n are the characteristic roots of the following equation:

$$\tan \mu + K_e \tan(K_2^{1/2} K_\delta \mu) = 0. \tag{15}$$

The equivalent thickness of the uniform gas lens, δ , can

be computed by referring to Fig. 3(a). The volume of the gas lens is

$$\left(\frac{\pi}{4} \right) d_c^2 h - \pi h^2 \left(\frac{d_p}{2} - \frac{1}{3} h \right) = \left(\frac{\pi}{4} \right) d_c^2 \delta, \tag{16}$$

where $h = 0.2938 d_c$. This finally gives

$$\delta = 0.13 d_c. \tag{17}$$

Substitution of δ from equation (17) into equation (14) yields K_δ as 7.7.

The average heat flux, q , between the heat transfer surface and the first row of particles through the gas film is

$$q = \frac{1}{\tau_1} \int_0^{\tau_1} -k_g \frac{\partial T_g(x, \tau)}{\partial x} \Big|_{x=-\delta} d\tau. \tag{18}$$

Substituting for the derivative from equation (11), we finally get after integration,

$$q = k_g T_w \left\{ \frac{1}{K_1 d_c + \delta} + \sum_{n=1}^{\infty} \frac{2K_e \delta \sin^2(m \mu_n)}{\alpha_g \tau_1 \mu_n^2 [K_e \sin^2(m \mu_n) + m \sin^2 \mu_n]} \times [1 - \exp(-\mu_n^2 \alpha_g \tau_1 / \delta^2)] \right\}. \tag{19}$$

The contribution of second and higher terms in the above series is very small ($\sim 1\%$) and therefore we can simplify equation (19) with very little error as

$$q = k_g T_w \left\{ \frac{1}{K_1 d_c + \delta} + \frac{2K_e \delta \sin^2(m \mu_1)}{\alpha_g \tau_1 \mu_1^2 [K_e \sin^2(m \mu_1) + m \sin^2 \mu_1]} \times [1 - \exp(-\mu_1^2 \alpha_g \tau_1 / \delta^2)] \right\}. \tag{20}$$

Further

$$q = h_{cond} (T_w - T_{gp}) \tag{21}$$

where T_{gp} is the average temperature of the composite layer of gas and particle, as shown in Fig. 2, and may be evaluated from equations (11) and (12) after retaining only the first term of the series. This gives

$$T_{gp} = \frac{T_w}{d_c + \delta} \left\{ \frac{K_1 d_c^2 + 2K_1 d_c \delta + \delta^2}{2(K_1 d_c + \delta)} - \frac{2\delta^3 K_e \sin^2(m \mu_1) (1 - \cos \mu_1)}{\tau_1 \alpha_g \mu_1^4 [K_e \sin^2(m \mu_1) + m \sin^2 \mu_1]} \times \left[1 - \exp\left(-\frac{\mu_1^2 \alpha_g \tau_1}{\delta^2}\right) \right] + \frac{2K_e \delta d_c^2 \sin \mu_1 \sin(m \mu_1)}{\tau_1 \alpha_p \mu_1^4 m^2 K_x^{1/2}} \times \frac{[1 - \cos(m \mu_1)]}{[K_e \sin^2(m \mu_1) + m \sin^2 \mu_1]} \times \left[1 - \exp\left(-\frac{\mu_1^2 m^2 \alpha_p \tau_1}{d_c^2}\right) \right] \right\}. \tag{22}$$

By combining equations (20)–(22), and neglecting the terms involving higher powers of μ_1 , we get the following expression within an estimated error of about 1.5%

$$h_{\text{cond}} = 1.06 \frac{k_g}{\delta} \left\{ 1 + \frac{K_\epsilon(1 + K_1 K_\delta)}{(K_\epsilon + m \sin^2 \mu_1) \mu_1^2 Fo} \times [1 - \exp(-\mu_1^2 Fo)] \right\}. \quad (23)$$

The numerical value of the second term in equation (23) depends upon the magnitude of the quantity $(1/\mu_1^2 Fo) [1 - \exp(-\mu_1^2 Fo)]$ which varies from 0 to 1. The maximum value 1 corresponds to $\tau_1 \rightarrow 0$. Even the analysis for this hypothetical case ($\tau \rightarrow 0$) shows that the contribution of the second term in equation (23) for all the gases except helium and hydrogen, in the temperature range 273–1100 K and pressure range 0.1–10 MPa, is always within 20% of the leading term. Thus equation (21) can be approximated within an estimated error of less than 20% by

$$h_{\text{cond}} = 1.06 (k_g/\delta). \quad (24)$$

This uncertainty in h_{cond} does not seem to be important in view of the difficulties in determining τ_1 . Also the contribution of h_{cond} to h_w for large particle systems is relatively small as compared to h_{conv} . In the general case, the heat transfer surface will not be completely covered with the bed particles and therefore h_{cond} must be modified to account for the bed voidage. If N is the number of particles on the unit area of the heat transfer surface, then the fraction of this unit surface covered with particles is $(\pi d_c^2/4)N$. Therefore

$$h_{\text{cond}} = 1.06(k_g/\delta) (\pi d_c^2/4)N. \quad (25)$$

Alternatively, it can be expressed in terms of the bed voidage, ϵ , as

$$h_{\text{cond}} = 1.02(k_g/\delta) (1 - \epsilon)^{2/3}. \quad (26)$$

Substituting for δ from equations (16) and (2)

$$h_{\text{cond}} = 8.95(k_g/\bar{d}_p) (1 - \epsilon)^{2/3} \quad (27)$$

or

$$Nu_{\text{cond}} = 8.95 (1 - \epsilon)^{2/3}. \quad (28)$$

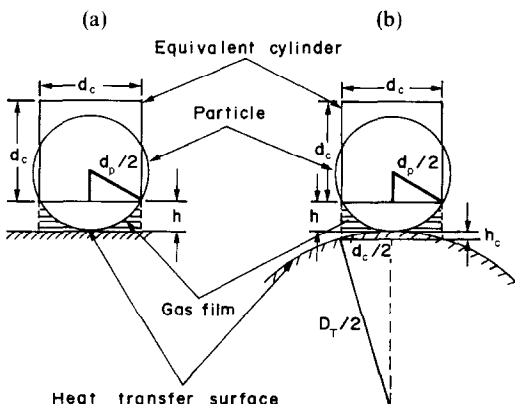


FIG. 3. Gas film thickness at the heat transfer surface.

In the above formulation, it has been assumed that the heat transfer surface is flat. However, in many applications related to coal conversion technology the heat transfer surfaces may have appreciable curvature. One such well known example is that of boiler tubes for either generating process steam or driving a steam turbine for power generation. It will, therefore, be interesting to examine the effect of such a curvature in the heat transfer surface on h_w . It is investigated here in the following.

The gas film thickness is larger for the case when the heat transfer surface has a curvature in comparison to a flat surface with no curvature. For a curved surface (Fig. 3b) the gas film thickness, δ_c , is given by

$$\delta_c = 0.114 \bar{d}_p + h_c - 5.24 \frac{h_c^2}{\bar{d}_p^2} \left(\frac{D_T}{2} - \frac{1}{3} h_c \right) \quad (29)$$

where h_c , as shown in the Fig. 3(b), is the maximum thickness of that part of the gas film lens which is due to the curvature of the heat transfer surface. It is zero for the case when the heat transfer surface is flat and otherwise is given by

$$h_c = \frac{1}{2} \left[D_T - (D_T^2 - 0.763 \bar{d}_p^2)^{1/2} \right]. \quad (30)$$

Combining equations (26) and (29), noting $\delta = \delta_c$,

$$Nu_{\text{cond}} = (1.02/k) (1 - \epsilon)^{2/3} \quad (31)$$

where

$$k = 0.114 + \frac{h_c}{\bar{d}_p} - \frac{5.24 h_c^2}{\bar{d}_p^3} \left(\frac{D_T}{2} - \frac{1}{3} h_c \right). \quad (32)$$

Since, in general, h_c can be regarded as being much smaller than \bar{d}_p and D_T , the third term on the RHS of equation (32) can be neglected, so that to a good degree of approximation

$$k \approx 0.114 + (h_c/\bar{d}_p). \quad (33)$$

Consequently, Nu_{cond} is finally given by

$$Nu_{\text{cond}} = \frac{1.02 (1 - \epsilon)^{2/3}}{[0.114 + (h_c/\bar{d}_p)]}. \quad (34)$$

Calculation of convective component, h_{conv}

For beds of large particles, the Reynolds number is invariably larger than 100 and the flow around the particles is turbulent [22]. The intensity of turbulence is known to be dependent on particle size and bed voidage [24]. It would, therefore, follow that the gas flow around a surface immersed in a fluidized bed of large particles is turbulent. The turbulent boundary layer formed on the immersed surface is continuously disturbed by the front half of the bed particles and formed again in their wake [25, 26]. The heat transfer surface may thus be regarded as covered with a continuous arrangement of unit orthorhombic cells which in time keeps reforming as new particles arrive at the surface. The heat transfer from the surface corresponding to each of these unit cells through the

turbulent boundary layer can be considered similar to that of a flat plate immersed in a turbulent gas stream. Other evidence supporting this view lies in the experimental measurements of Borodulya *et al.* [15], and Rabinovich and Sachenov [27] on heat transfer studies from immersed surfaces at high pressures in fluidized beds of large particles. These authors [15, 27] found that the dependence of the heat transfer coefficient on the Reynolds number is somewhat similar and their values of the exponents are in good agreement with the values found for flat plates.

The heat transfer from a plate placed in a turbulent fluid flow is given by

$$(Nu_l)_{conv} = C Re_l^{0.8} Pr^{0.43} \quad (35)$$

where Nu_l and Re_l are based on the characteristic length parameter [28, 29]. The characteristic length parameter for calculating Nu_l and Re_l in equation (35) for fluidized bed heat transfer needs to be defined. To accomplish this let us refer to Fig. 1, when l for such a unit orthorhombic particle arrangement is given by

$$l = \frac{4}{\pi d_c} \left[\int_{\theta}^{(L-d_c)/2} \left\{ [(d_c^2/4) - x^2]^{1/2} + 3^{1/2} L \right\} dx \right. \\ \left. + \int_{-d_c/2}^{(d_c-L)/2} \left\{ [(d_c^2/4) - x^2]^{1/2} \right. \right. \\ \left. \left. + (3^{1/2}/2) L \right\} dx - (\pi/16) d_c^2 \right] \quad (36)$$

which gives

$$l = 3^{1/2} L^2 / \pi d_c. \quad (37)$$

Substituting for L and d_c from equations (3) and (2) respectively

$$l = 0.63 \bar{d}_p \left(\frac{1 - \bar{\epsilon}}{1 - \epsilon} \right)^{2.3}. \quad (38)$$

As stated earlier, $\bar{\epsilon} = 0.395$ so that

$$l = 0.451 \bar{d}_p (1 - \epsilon)^{-2.3}. \quad (39)$$

Equation (35) in conjunction with equation (39) gives

$$Nu_{conv} = C_0 Re^{0.8} Pr^{0.43} \left[\frac{(1 - \epsilon)^{0.133}}{\epsilon^{0.8}} \right] \quad (40)$$

where

$$C_0 = 1.173 C. \quad (41)$$

The constant C is determined experimentally and is discussed in the next section.

The total heat transfer coefficient in accordance with equation (1) can now be written in terms of the Nusselt number as follows:

$$Nu_p = Nu_{cond} + Nu_{conv}. \quad (42)$$

The particle Nusselt number, $Nu_p = h_w \bar{d}_p / k_g$, for the case of a flat heat transfer surface is

$$Nu_p = 8.95 (1 - \epsilon)^{0.667} + C_0 Re^{0.8} Pr^{0.43} \\ \times \left[\frac{(1 - \epsilon)^{0.133}}{\epsilon^{0.8}} \right] \quad (43)$$

and for the case of a curved surface is

$$Nu_p = \frac{1.02 (1 - \epsilon)^{0.667}}{\{0.114 + (h_c / \bar{d}_p)\}} + C_0 Re^{0.8} Pr^{0.43} \\ \times \left[\frac{(1 - \epsilon)^{0.133}}{\epsilon^{0.8}} \right]. \quad (44)$$

The constant C_0 can be obtained if simultaneous measurements of h_w and ϵ are made. We performed such experiments with a single 13 mm dia vertical tube and its staggered bundles in a restricted bed at high gas velocities. This gave a mean value of 0.12.

ϵ in the above relations is the bed voidage near the heat transfer surface and this value is larger than the bulk bed voidage. Kimura and Kaneda [30] have determined the distribution of voidage in packed beds and found that the bed voidage variation is limited to a region of about half a particle diameter from the surface. Denloye [31] employed their [30] correlation to develop the following relationship for a quiescent fluidized bed:

$$\epsilon_w = 1 - \frac{(1 - \bar{\epsilon}) [0.7293 + 0.5139 (\bar{d}_p / D_T)]}{[1 + (\bar{d}_p / D_T)]}. \quad (45)$$

Here, ϵ_w and $\bar{\epsilon}$ are the bed voidage values near the surface and the bulk of the bed respectively. We have used this relation to calculate ϵ_w at minimum fluidization condition.

As the fluidization commences, the bed voidage near the surface changes more rapidly than in the bulk of the bed in the beginning. This is due to the larger gas flow near the surface owing to the larger bed voidage than in the bulk of the bed. At higher gas flows, this rate of voidage change becomes slower because of the frictional resistance offered to the bed expansion by the immersed surface. Based on our experience with bed expansion measurements currently in progress, we propose to express the variation of ϵ with G (or Re) as

$$\epsilon = \epsilon_w + 1.65 A (1 - \bar{\epsilon}) [1 - \exp(-a/A^2)]. \quad (46)$$

Here $\bar{\epsilon}$ is the bed voidage at minimum fluidization, a is $\{0.367 \ln[(\epsilon_w - \bar{\epsilon})/(1 - \bar{\epsilon})]\}$ and

$$A = (Re - Re_{mf}) / Ar^{0.5}. \quad (47)$$

The relation of equation (46) is employed to compute the bed voidage near the heat transfer surface at any fluidization velocity, G , for use in equations (43) and (44).

In the above calculation Nu_p employs a value of C_0 which is obtained on the basis of experimental data for heat transfer tubes of diameter 13 mm. A small correction must be applied to the Nusselt number obtained for tubes of different diameter according to the following relation:

$$(Nu_p)_{D_1} = \\ (Nu_p)_{13\text{mm}} \frac{\{1 - \exp[-0.1 Ar^{0.1} (13/\bar{d}_p(\text{mm}))]\}}{\{1 - \exp[-0.1 Ar^{0.1} (D_T/\bar{d}_p)]\}}. \quad (48)$$

This semi-empirical correction is obtained on the basis

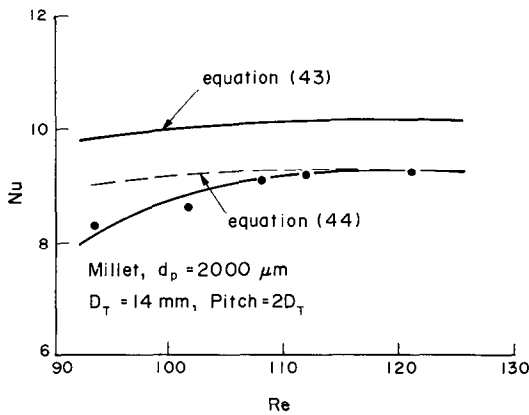


FIG. 4. Comparison of experimental data [14] for horizontal equilateral triangular tube bundle with the present theory.

of observed variation of the maximum value of the Nusselt number with tube diameter [17].

COMPARISON OF THEORY WITH EXPERIMENT

A search of the literature revealed that several sets of experimental data dealing with single tubes and tube bundles with widely spaced tubes are available for checking the appropriateness of the theory developed here [11, 13, 14, 32, 33]. All these data sets are considered here with the results reported below. In all cases the experimental heat transfer data are considered in terms of the Nusselt number and its variation with the Reynolds number. Two variants of the present theory calculations are discussed, the first by considering the heat transfer surface to be flat [equation (43)] and the second in which allowance has been made for the curvature of the surface [equation (44)]. In the figures referred to below the continuous and dashed curves are according to equations (43) and (44) respectively.

In Fig. 4, the experimental data [14] for a bed of millet ($\bar{d}_p = 2000 \mu\text{m}$) and a staggered bundle of 14 mm tubes arranged in an equilateral triangular arrangement with pitch equal to $2D_T$ under ambient conditions are shown. The calculated values taking into account the tube curvature are in excellent agreement with the measured values. The neglect of curvature produces values which are about 10% larger than those which do consider the tube curvature. The curvature correction is appreciable because the tube diameter is small and particle diameter is large, i.e. \bar{d}_p/D_T is large.

A similar comparison for the experimental data of ref. [11] with the present theory is given in Fig. 5. The data are taken under ambient conditions with a single 50.8 mm tube immersed in fluidized beds of glass beads ($\bar{d}_p = 4000 \mu\text{m}$) and dolomite ($\bar{d}_p = 1300 \mu\text{m}$). The agreement between theory and experiment is good and in general the deviation is of the order of 10%. The calculations taking into account the tube curvature lead to values which are about 2% smaller than the values which neglect curvature. The small difference in the two sets of computed values is due to the small value of the \bar{d}_p/D_T ratio.

The data of ref. [32] taken with a single tube of 28.6 mm immersed in a fluidized bed of soda lime glass beads ($\bar{d}_p = 1580 \mu\text{m}$) under ambient conditions are displayed in Fig. 6. The theory again reproduces the experimental data within an average deviation of about 10%. However, the qualitative trend of experimental values being smaller than the calculated values, evident to some extent in the previous case [11], is clear in this case. The tube curvature correction follows the same trend as in the two previous cases (Figs. 4 and 5) and its magnitude is about 4%.

Experimental results [33] for dolomite particles ($\bar{d}_p = 1300 \mu\text{m}$) and a bundle of 101.6 mm tubes arranged in an equilateral arrangement of pitch $2D_T$ at atmospheric pressure and four temperature levels in the

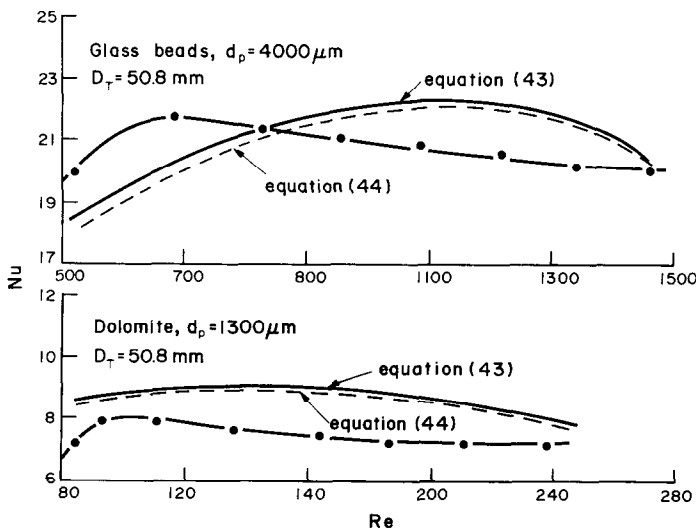


FIG. 5. Comparison of experimental data [11] for single horizontal tube with the present theory.

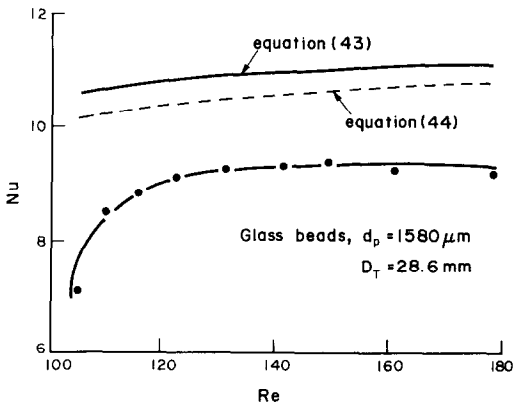


FIG. 6. Comparison of experimental data [32] for single horizontal tube with the present theory.

range 274–649 K are plotted in Fig. 7. The theoretical predictions, dashed curves, are in good agreement with the observed data except at the highest temperature. However, the scatter in the data excludes any other precise conclusion. The curvature correction seems to improve the agreement of theory with the experiment, though the correction is small (about 2%) in view of the small value of \bar{d}_p/D_T ratio. From this comparison as with the earlier ones to some extent, it follows that the theory is capable of reproducing the dependence of the Nusselt number on the Reynolds number. One important point to note in this comparison is the fact that the Reynolds number is always smaller than 60 and according to the established practice [22, 23] the flow regime is transitional for $20 < Re < 60$, the range covered by ref. [33]. It seems, therefore, likely that the present theory developed for turbulent regime is reasonably good even for transitional regime $10 < Re < 100$.

Figures 8 and 9 exhibit the data [13] for millet ($\bar{d}_p = 2000 \mu\text{m}$) and fire clay ($\bar{d}_p = 3000 \mu\text{m}$) respectively for a staggered tube bundle in which 30 mm tubes are located on the vertices of an equilateral triangular configuration of pitch 45 and 60 mm under ambient conditions of temperature and pressure. In both the

cases, the present theory with curvature correction can predict the experimental data with good accuracy both in regards to its magnitude as well as the variation of Nu with Re . The curvature correction which is only about 3% does make a difference in improving the agreement between theory and experiment.

On the basis of the above detailed comparison of theory and experiment, it is possible to draw the following conclusions:

(1) The present theory developed for heat transfer between immersed surfaces and fluidized beds of large particles is successful in correlating and reproducing all the available experimental data for such systems with good accuracy. It should, therefore, provide a good base for design and prediction purposes.

(2) The calculations reveal that the consideration of the curvature of the heat transfer surface while computing the conduction component of the heat transfer coefficient improves the prediction potential of the theory and these values, in general, are in better agreement with the experimental values than those which neglect the curvature of the surface. The curvature correction depends upon the value of the diameter ratio, \bar{d}_p/D_T . The larger the magnitude of this ratio, the larger the correction. Consequently for larger particles, when experiments are conducted in subpilot studies with small diameter boiler tubes, this correction must be included.

(3) This theory is unique amongst all the available ones in reproducing the dependence of h or Nu on G or Re . However, a more crucial check of the proposed theory will be in order with the availability of experimental data over a wide range of Reynolds number. Certainly a body of accurate data covering a wide range of Reynolds number will be useful for broadening the scope of the proposed theory, establishing its reliability, and in exploring those aspects which need refinement and reformulation. In this context the evaluation of ϵ and C_0 need special attention.

Acknowledgement—This research is supported in part by the United States National Science Foundation in a collaborative research program between the U.S.A. and U.S.S.R.

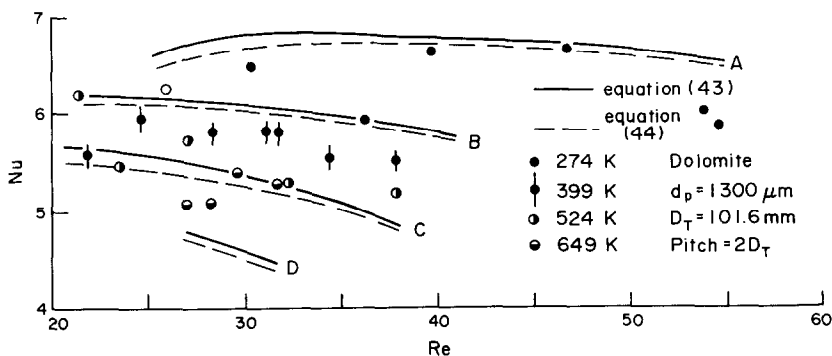


FIG. 7. Comparison of experimental data [33] for horizontal equilateral triangular tube bundle with the present theory.

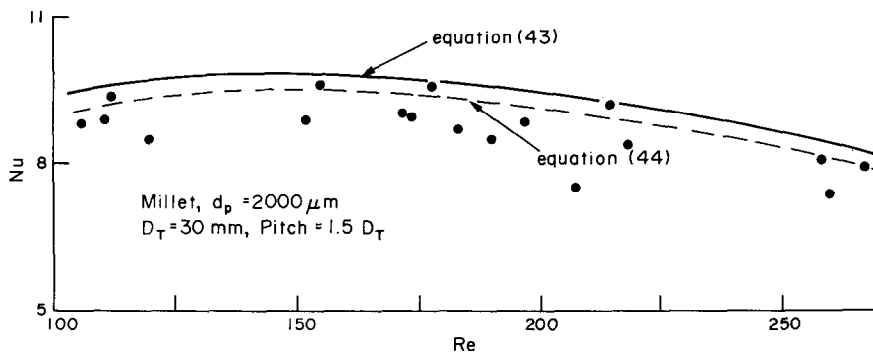


FIG. 8. Comparison of experimental data [13] for horizontal equilateral triangular tube bundle with the present theory.

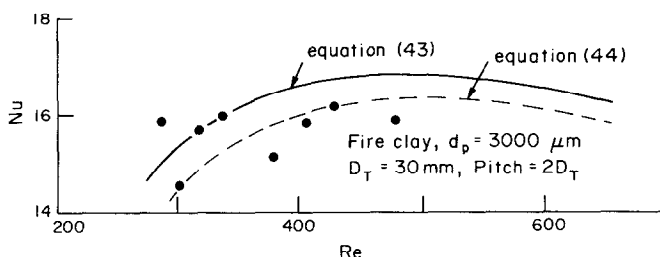


FIG. 9. Comparison of experimental data [13] for horizontal equilateral triangular tube bundle with the present theory.

REFERENCES

1. A. P. Baskakov, *Heat and Mass Transfer Processes in a Bubbling Fluidized Bed*. Metallurgia, Moscow (1978).
2. J. S. M. Botterill, *Fluid-Bed Heat Transfer*. Academic Press, New York (1978).
3. S. C. Saxena, N. S. Grewal, J. D. Gabor, S. S. Zabrodsky and D. M. Galershtein, Heat transfer between a gas fluidized bed and immersed tubes, in *Advances in Heat Transfer* (edited by T. F. Irvine, Jr. and J. P. Hartnett) **14**, 149–247 (1978).
4. S. C. Saxena and J. D. Gabor, Mechanisms of heat transfer between a surface and a gas-fluidized bed for combustor application, *Prog. Energy Combust. Sci.* to be published (1982).
5. N. M. Catipovic, G. N. Jovanovic and T. J. Fitzgerald, Regimes of fluidization for large particles, *A.I.Ch.E. JI* **24**, 543–547 (1978).
6. C. S. Canada, M. D. McLaughlin and F. W. Staub, Flow regimes and void fraction distribution in gas fluidization of large particles without tube banks, *A.I.Ch.E. Symp. Ser.* **74**, 14–26 (1976).
7. J. Yerushalmi, D. H. Turner and A. M. Squires, The fast fluidized bed, *I/EC Proc. Des. Dev.* **15**, 47–53 (1976).
8. V. K. Maskaev and A. P. Baskakov, Characteristics of external heat transfer in fluidized beds of coarse particles, *Inzh-Fiz. Zhurn.* **24**, 589–593 (1972).
9. A. O. O. Denloye and J. S. M. Botterill, Bed to surface heat transfer in a fluidized bed of large particles, *Powder Technol.* **19**, 197–203 (1978).
10. F. W. Staub, Solids circulation in turbulent fluidized beds and heat transfer to immersed tube banks, *Trans. Am. Soc. Mech. Engrs. Series C, J. Heat Transfer* **101**, 391–396 (1979).
11. N. M. Catipovic, G. N. Jovanovic, T. J. Fitzgerald and O. Levenspiel, A model for heat transfer to horizontal tubes immersed in a fluidized bed of large particles, in *Fluidization* (edited by J. R. Grace and J. M. Matsen) pp. 225–234. Plenum Press, New York (1980).
12. L. R. Glicksman and N. Decker, Heat transfer in fluidized beds with large particles, *Proc. 6th Int. Conf. Fluidized Bed Combustion*, 9–11 April, Atlanta, Georgia, U.S.A., Vol. III-Technical Sessions, pp. 1152–1158 (1980).
13. S. S. Zabrodsky, Yu. G. Epanov, D. M. Galershtein, S. C. Saxena and A. K. Kolar, Heat transfer in a large particle fluidized bed with immersed in-line and staggered bundles of horizontal smooth tubes, *Int. J. Heat Mass Transfer* **24**, 571–579 (1981).
14. V. A. Borodulya, V. L. Ganzha, S. N. Upadhyay and S. C. Saxena, Heat transfer from in-line and staggered horizontal smooth tube bundles immersed in a fluidized bed of large particles, *Int. J. Heat Mass Transfer* **23**, 1602–1604 (1980).
15. V. A. Borodulya, V. L. Ganzha and A. I. Podberezhsky, Heat transfer in a fluidized bed at high pressure, in *Fluidization* (edited by J. R. Grace and J. M. Matsen) pp. 201–207. Plenum Press, New York (1980).
16. G. S. Canada and M. H. McLaughlin, Large particle fluidization and heat transfer at high pressures, *A.I.Ch.E. Symp. Ser.* **74**, No. 176, 27–37 (1976).
17. V. A. Borodulya, V. L. Ganzha and A. I. Podberezhsky, Surface-to-bed heat transfer in a large particle fluidized bed, *Problemy Teple-i-Massoobmena v Processach Gorennya, Ispolzuemych v Energetice*, Minsk, pp. 141–157 (1980).
18. A. K. Kolar, N. S. Grewal and S. C. Saxena, Investigation of radiative contribution in a high temperature fluidized-bed using the alternate-slab model, *Int. J. Heat Mass Transfer* **22**, 1695–1703 (1979).
19. D. Geldart, Types of gas fluidization, *Powder Technol.* **7**, 285–292 (1973).
20. A. M. Xavier, D. F. King, J. F. Davidson and D. Harrison, Surface-to-bed heat transfer in a fluidized bed at high pressure, in *Fluidization* (edited by J. R. Grace and J. M.

- Matsen) pp. 209–216. Plenum Press, New York (1980).
21. A. V. Luikov, *Theory of Thermal Conductivity* (in Russian) pp. 288–290. Gostechizdat, Moscow (1952); English translation, *Analytical Heat Diffusion Theory* (edited by J. P. Hartnett) pp. 411–417. Academic Press, New York (1968).
 22. M. Leva, *Fluidization*, p. 49. McGraw–Hill, New York (1959).
 23. M. E. Aerov and O. M. Todes, *Hydraulic and Thermal Fundamentals of the Operation of Steady-State and Fluidized Bed Granular Bed Apparatus*. p. 510. L. Khimiya (1968).
 24. T. R. Galloway and B. H. Sage, A model of the mechanism of transport in packed, distended and fluidized beds, *Chem. Engng Sci.* **30**, 495–516 (1970).
 25. O. Levenspiel and J. S. Walton, Bed-wall heat transfer in fluidized systems, *Chem. Engng Prog. Symp. Ser.* **50**, No. 9, 7–13 (1954).
 26. D. T. Wasan and K. S. Ahluwalia, Consecutive film and surface renewal mechanisms for heat or mass transfer from wall, *Chem. Engng Sci.* **24**, 1535–1542 (1969).
 27. L. B. Rabinovitch and G. P. Sechenov, Study of conditions of heat transfer from surface to fluidized beds under pressure, *Eng. Phys. Zh.* (Russian), **22**, 789–794 (1972).
 28. F. P. Incropera and D. P. DeWitt, *Fundamentals of Heat Transfer* pp. 328–330. John Wiley, New York (1981).
 29. V. P. Isachenko, O. A. Osipova and A. S. Sukomel, *Heat Transfer*. p. 209. Mir, Moscow (1977).
 30. M. Kimura, K. Nono and T. Kaneda, Distribution of void in packed tube, *Chem. Engng Japan* **19**, 397–900 (1955).
 31. A. O. O. Denloye, Ph.D. Thesis, University of Birmingham, U.K. (1976) cited in A. O. O. Denloye and J. S. M. Botterill, A theoretical model of heat transfer to a packed or quiescent fluidized bed, *Chem. Engng Sci.* **33**, 509–515 (1978).
 32. R. Chandran, J. C. Chen and F. W. Staub, Local heat transfer coefficient around horizontal tubes in fluidized beds, *Trans. Am. Soc. Mech. Engrs, Series C, J. Heat Transfer* **102**, 152–157 (1980).
 33. L. P. Golon, G. V. LaLonde and S. C. Weiner, High temperature heat transfer studies in a tube filled bed, *Proc. 6th Int. Conf. Fluidized Bed Combustion*. 9–11 April, Atlanta, Georgia, U.S.A., pp. 1173–1185 (1980).

UNE THEORIE MECANIQUE DU TRANSFERT THERMIQUE ENTRE DES LITS FLUIDISES DE PARTICULES GROSSES ET DES SURFACES IMMERGEES

Résumé—On développe une théorie mécanique du transfert thermique entre une surface immergée et un lit fluidisé de grosses particules, en adoptant l'idée bien acceptée qu'en l'absence de rayonnement le coefficient de transfert thermique total est la somme d'une composante conductive (h_{cond}) et d'une convective (h_{conv}). Les solides sont supposés distribués autour de la surface selon un arrangement de cellules orthorhombic. On calcule h_{cond} en considérant une couche composite de gaz et de solide et en résolvant les equations de la conduction de chaleur en régime permanent avec des conditions bien définies aux limites et initiale. On évalue h_{conv} en supposant que la couche limite turbulente sur la surface est interrompue dans le plan milieu de la particule et qu'elle se reforme dans le sillage. Les résultats du calcul pour le coefficient total de transfert thermique sont en bon accord avec les données expérimentales disponibles pour des systèmes de grandes particules. La théorie proposée est considérée comme un bon moyen de prédiction pratique.

EINE MECHANISTISCHE THEORIE FÜR DEN WÄRMEÜBERGANG ZWISCHEN WIRBELSCHICHTEN AUS GROSSEN PARTIKELN UND DARIN EINGETAUCHTEN OBERFLÄCHEN

Zusammenfassung—Eine mechanistische Theorie für den Wärmetransport zwischen einem Wirbelbett aus großen Partikeln und einer darin eingetauchten Oberfläche wird unter Verwendung des bekannten Ansatzes, daß der Gesamtwärmeübergangs-Koeffizient, falls keine Strahlung auftritt, die Summe aus der Leitungs- (h_{cond}) und der Konvektionskomponente (h_{conv}) ist, dargelegt. Es wird angenommen, daß die Festkörper um die wärmeabgebende Oberfläche in einer Anordnung von orthorhombischen Einheitszellen verteilt sind. Betrachtet man eine aus Gas und Festkörpern zusammengesetzte unendliche Schicht, so kann h_{cond} durch Lösen der instationären Wärmeleitgleichung bei bekannten Rand- und Anfangsbedingungen berechnet werden. Durch die Annahme, daß die turbulente Grenzschicht der Wärmeübertragungsfläche an der vorderen Hälfte der Partikel aufgerissen wird und sich im Nachlauf wieder neu bildet, läßt sich h_{conv} bestimmen. Die theoretischen Modellberechnungen stimmen gut mit den verfügbaren experimentellen Daten grobkörniger Systeme überein. Die vorgelegte Theorie wird als gute Grundlage für Auslegung und Berechnung betrachtet.

МЕХАНИЧЕСКАЯ ТЕОРИЯ ТЕПЛООБМЕНА МЕЖДУ ПСЕВДООЖИЖЕННЫМ СЛОЕМ КРУПНЫХ ЧАСТИЦ И ПОГРУЖЕННЫМИ ПОВЕРХНОСТЯМИ

Аннотация—Предложена механическая теория теплообмена между псевдоожигенным слоем крупных частиц и погруженными поверхностями, основанная на известной концепции о рассмотрении коэффициента теплообмена как суммы кондуктивной ($h_{\text{конд}}$) и конвективной ($h_{\text{конв}}$) (при отсутствии лучистой) составляющих. Принята орторомбическая укладка частиц у теплообменной поверхности. Величина $h_{\text{конд}}$ определена путем использования решения нестационарной задачи о прогреве пакета, состоящего из двух слоев: газа и твердого материала. Величина $h_{\text{конв}}$ рассчитывается, исходя из предположения о существовании турбулентного пограничного слоя у теплообменной поверхности, формирующегося заново после каждой частицы. Рассчитанные по соотношениям, полученным на основе предложенной модели, коэффициенты теплообмена хорошо согласуются с имеющимися в литературе экспериментальными данными.